

10

Strong coupling

In the statistical analog, the strong coupling regime is the high temperature limit. High temperature expansions are an old subject in solid state physics, but before Wilson's work they were relatively unknown to particle theorists. Indeed, in the continuum theory the strong coupling limit is rather unnatural and difficult to treat. In contrast, on the lattice strong coupling is by far the simplest limit. One merely expands the Boltzmann factor in powers of the inverse temperature and evaluates the terms in the resulting series. In the gauge theory each power of β is associated with a plaquette somewhere in the lattice. This gives a simple diagrammatic interpretation in terms of graphs built up from such plaquettes (Wilson, 1974; 1975; Balian, Drouffe and Itzykson, 1975*b*).

We begin our discussion with a rectangular Wilson loop in pure $SU(n)$ lattice gauge theory without fermions

$$W(I, J) = Z^{-1} \int (dU) e^{-S} (1/n) \text{Tr} \prod_{ij \in C} U_{ij}. \quad (10.1)$$

Here the curve C is the rectangle of dimensions I by J in lattice units, and the factor of $1/n$ is inserted for convenience. As usual, the group elements are ordered as encountered in circumnavigating the contour. In figure 10.1 we show such a curve for a three-by-three loop. Because the variables become random in the strong coupling limit, it is simplest to shift the action by a constant from the normalization used in eq. (7.6). Thus we take

$$\begin{aligned} S &= -\sum_{\square} (\beta/n) \text{Re Tr } U_{\square} \\ &= -\sum_{\square} (\beta/(2n)) (\text{Tr } U_{\square} + \text{Tr } U_{\square}^*). \end{aligned} \quad (10.2)$$

We now observe that because

$$\int (dU) U_{ij} = 0 \quad (10.3)$$

all Wilson loops will vanish as β goes to zero. Indeed, for each link in the contour we must bring down at least one corresponding link from an expansion of the exponential of the action if we are to avoid the zeros from

eq. (10.3). Correspondingly, every link from the action must have a partner, either from the action itself or the inserted loop. The first non-vanishing contribution in the strong coupling series comes from tiling the loop with plaquettes as shown in figure 10.2. Note the orientations of the loops in the figure; this is important for all $SU(n)$ except $SU(2)$, for

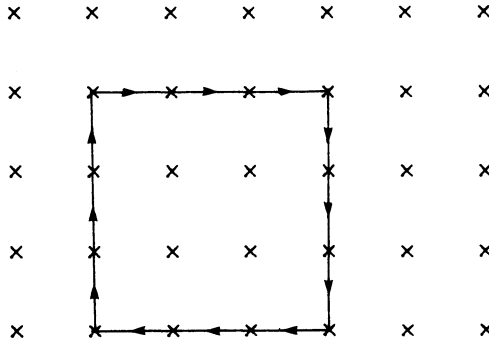


Fig. 10.1. A three-by-three Wilson loop.

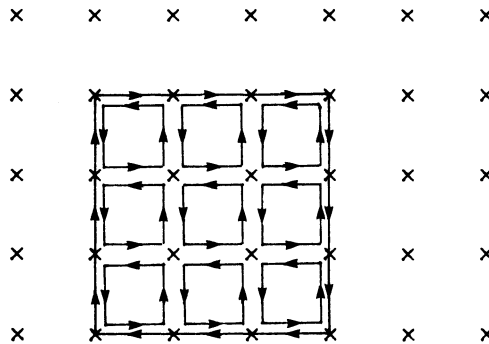


Fig. 10.2. Tiling the loop with plaquettes.

which $\text{Tr } U_{\square}$ is real. The simple integrals needed to evaluate this diagram are

$$\int dg 1 = 1 \tag{10.4}$$

for links outside the tiled region and

$$\int dg U_{ij} U_{kl}^{-1} = (1/n) \delta_{il} \delta_{jk} \tag{10.5}$$

within the loop. These integrals can all be combined graphically using the rules from the chapter on group integration. We obtain a factor of n^{-1} from each pair of bond variables and a factor of n from each site on the surface,

including the boundary. Multiplying these with $\beta/(2n)$ for each plaquette brought down from the exponential of the action, we obtain the result

$$W(I, J) \xrightarrow{\beta \rightarrow 0} \begin{cases} (\beta/(2n^2))^{IJ}, & n > 2 \\ (\beta/4)^{IJ}, & SU(2). \end{cases} \quad (10.6)$$

The difference for $SU(2)$ arises from the non-oriented nature of the plaquettes.

At this lowest non-trivial order of strong coupling we already see an area law

$$W(I, J) \sim e^{-KA}, \quad (10.7)$$

where the area in physical units is

$$A = a^2 IJ \quad (10.8)$$

and the string tension starts out

$$K \xrightarrow{\beta \rightarrow 0} \begin{cases} -a^{-2} \log(\beta/(2n^2)), & n > 2 \\ -a^{-2} \log(\beta/4), & SU(2). \end{cases} \quad (10.9)$$

This area law behavior will persist for arbitrarily shaped loops. The leading contribution in the small β limit always follows from tiling the minimal surface bounded by the loop.

The existence of an area law behavior for the Wilson loop is a nearly universal phenomenon in the strong coupling limit. It occurs for all gauge groups in which no singlets appear in the direct product of the fundamental representation with any number of adjoint representations. This includes most but not all groups of interest. In physical terms, if a finite number of gluons can neutralize a source in the fundamental representation, then they will surround the edge of the large Wilson loop and give a perimeter law type of behavior. This occurs with the group $SO(3)$ where a singlet occurs in the product of three spin-one representations. For large loops the leading strong coupling diagram is sketched in figure 10.3. This is a purely gluonic analog of the phenomenon discussed in chapter 9, where we argued that the area law is no longer a useful order parameter after quarks enter the theory.

To keep from writing equations for several cases, we now restrict ourselves to the group $SU(3)$. Then the next contribution arises from replacing one of the tiling plaquettes with two of the opposite orientation. The resulting diagram appears in figure 10.4. The new integrals follow from eq. (8.56) of the chapter on group integration. Allowing for the insertion to be placed anywhere on the tiled surface, we obtain

$$W(I, J) = (\beta/18)^{IJ} (1 + IJ\beta/12 + O(\beta^2)), \quad (10.10)$$

$$a^2 K = -\log(\beta/18) - \beta/12 + O(\beta^2). \quad (10.11)$$

Note that this particular correction to the leading order has the same geometric structure. We still consider the tiling of a minimal surface inside the loop and have only introduced a new type of tile. A simple change of variables permits the summation of all contributions of this type. Consider

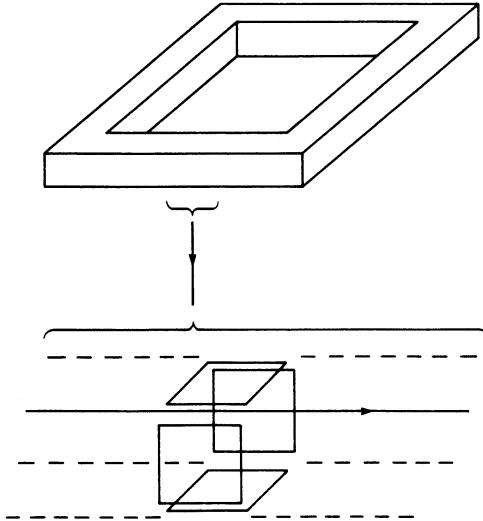


Fig. 10.3. A strong coupling diagram for $SO(3)$ gauge theory. This contribution falls exponentially with the perimeter of the loop.

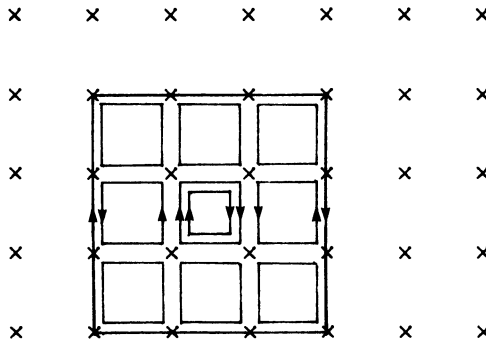


Fig. 10.4. A new type of tile.

the character expansion of the exponentiated plaquette operator

$$\exp(\frac{1}{3}\beta \text{Re Tr } U_{\square}) = N(\beta) (1 + \sum_{R \neq 1} b_R(\beta) \chi_R(U_{\square})). \quad (10.12)$$

Here the sum extends over all non-trivial irreducible representations of the group and χ_R is the trace or character in the corresponding representation. This sum is easily inverted using the orthogonality of the characters

(eq. 8.31), with the result

$$N(\beta) = \int dU \exp\left(\frac{1}{3}\beta \operatorname{Re} \operatorname{Tr} U\right), \quad (10.13)$$

$$b_R(\beta) = N^{-1} \int dU (\chi_R U)^* \exp\left(\frac{1}{3}\beta \operatorname{Re} \operatorname{Tr} U\right). \quad (10.14)$$

Using eq. (10.12), one replaces a sum over arbitrary powers of $\operatorname{Tr} U_\square$ on any given plaquette with a sum over representations of the group, each occurring only once. For low orders in the strong coupling expansion one can rapidly perform the needed group integrals with the use of familiar combination rules to form singlets from the representations appearing on the adjacent plaquettes to any given link. The disadvantage of this method is that as the order increases we must keep track of higher and higher representations.

We will now illustrate this technique with an evaluation of the string tension a^2K to an effective order β^6 . For $SU(3)$ the first few coefficients in eq. (10.12) are

$$b_3 = b_{\bar{3}} = \beta/6 + O(\beta^2), \quad (10.15)$$

$$b_6 = b_{\bar{6}} = \beta^2/72 + O(\beta^3) = b_3^2/2 + O(b_3^3), \quad (10.16)$$

$$b_8 = \beta^2/36 + O(\beta^3) = b_3^2 + O(b_3^3). \quad (10.17)$$

Higher representations start with higher powers of β . To avoid needing further terms in eq. (10.15), we express the result in powers of b_3 . Note that the normalization $N(\beta)$ drops out of the calculation due to the division by Z in expectation values. As before, the leading term for our flat Wilson loop arises from tiling the minimal surface with fundamental plaquettes. Thus eq. (10.9) becomes

$$a^2K \xrightarrow{\beta \rightarrow 0} -\log(b_3/3). \quad (10.18)$$

However now we encounter no corrections to this formula until order b_3^4 . This next term comes from a non-minimal tiled surface obtained by placing a cubical bump on our tiled plane as shown in figure 10.5. This adds four new plaquettes to the surface and we find

$$W(I, J) = (b_3/3)^{I+J} (1 + 4IJ(b_3/3)^4 + O(b_3^5)), \quad (10.19)$$

$$a^2K = -\log(b_3/3) + 4(b_3/3)^4 + O(b_3^5). \quad (10.20)$$

The factor of four in front of the new term represents the fact that the bump on our surface can either project above or below the plane in either of the two remaining dimensions of our four-dimensional space-time.

The next contribution arises from the same basic picture as in figure 10.5 but now with a non-trivial representation for the base of the cube. If we put a ‘floor’ on the bump using the $\bar{3}$ representation and reverse the

orientation of all plaquettes in the cap, we find

$$a^2 K = -\log(b_3/3) + 4(b_3/3)^4 + 12(b_3/3)^5 + O(b_3^6). \quad (10.21)$$

With the bump's floor in the sextet or octet representations, and with an appropriately oriented cap, we obtain contributions proportional to b_6 or b_8 multiplied by b_3^4 . By eq (10.16, 17) these terms are effectively of order b_3^6 .

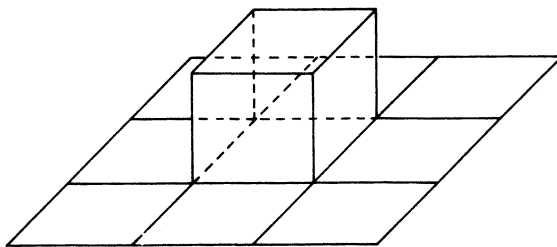


Fig. 10.5. An order b_3^4 correction to the string tension.

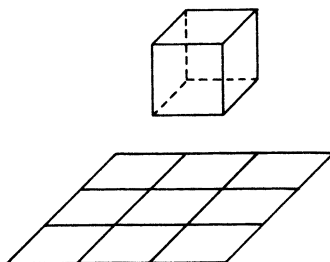


Fig. 10.6. A disconnected diagram.

At order b_3^6 a new type of contribution arises from the division by Z in evaluating expectation values. The partition function itself is a sum over disconnected diagrams. It serves to cancel diagrams with non-trivial representations on clusters of plaquettes completely isolated from the sources in the Wilson loop. For example, the diagram in figure 10.6 need not be evaluated. However, the division also removes some extra pieces if the cluster contributing to Z overlaps the connected numerator diagram. This gives a negative $O(b_3^6)$ contribution to the string tension, as illustrated in figure 10.7.

To complete the sixth-order strong coupling expansion for the string tension, we also must include the non-minimal bump illustrated in figure 10.8. Combining all contributions, we obtain

$$a^2 K = -\log(b_3/3) + 4(b_3/3)^4 + 12(b_3/3)^5 - 10(b_3/3)^6 + O(b_3^7). \quad (10.22)$$

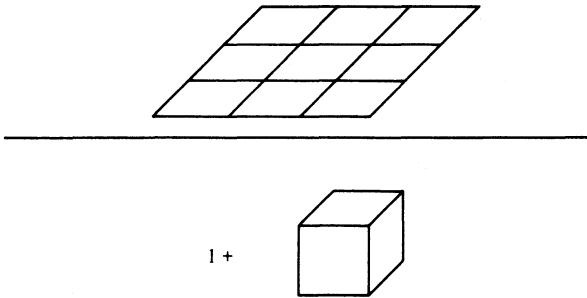


Fig. 10.7. A contribution from the division by Z.

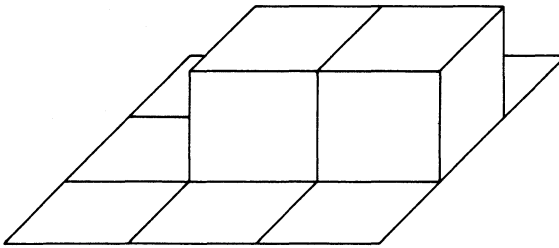


Fig. 10.8. A larger bump on the tiled surface.

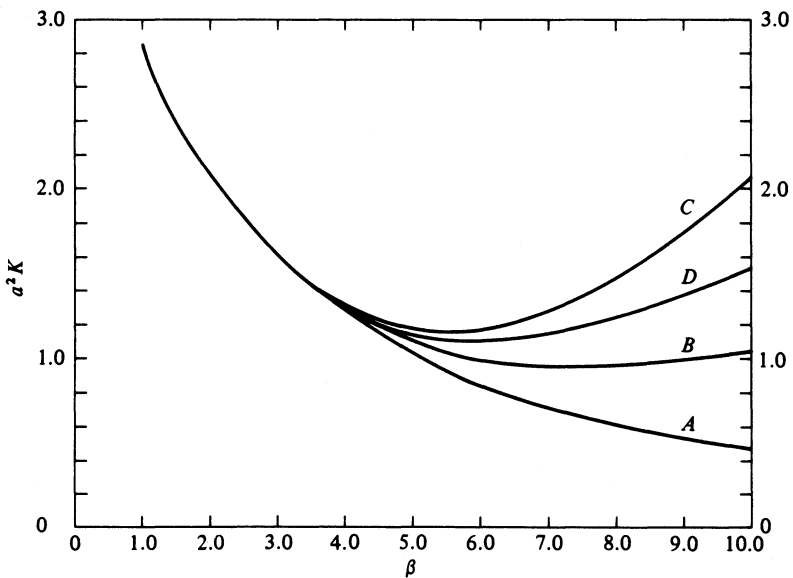


Fig. 10.9. The first few strong coupling approximations to the string tension. The curves A, B, C, and D respectively correspond to order 3, 4, 5, and 6 in powers of b_3 .

Beyond this order the calculation becomes rapidly more tedious. Munster and Weisz (1980) have evaluated the coefficients to order b_3^{12} .

In figure 10.9 we plot the first four strong coupling expressions for a^2K as functions of the basic inverse charge β . Note that for β less than five the result appears rather stable. This suggests that the radius of convergence of the strong coupling series is of order five. Indeed, the theory is known to be analytic in the vicinity of vanishing β (Osterwalder and Seiler, 1978). This contrasts with the usual perturbative expansion in coupling, which is known to be at best asymptotic (Dyson, 1952; Lipatov, 1977; Brezin, Le Guillou and Zinn-Justin, 1977*a, b*).

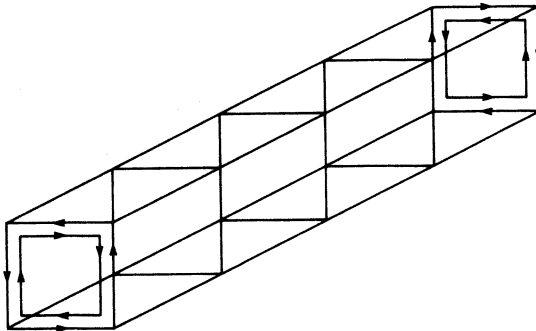


Fig. 10.10. A strong coupling diagram for calculating the mass gap. The sides of the square tube are to be tiled with fundamental plaquettes.

In this purely gluonic theory another interesting quantity for strong coupling studies is the mass gap. This is most easily extracted from the exponential decay of the correlation between two plaquettes separated by a large distance. Thus we effectively study the effects of glueball exchange between two gauge-invariant operators. To leading order we have the diagram shown in figure 10.10, where the tube connecting the end plaquettes is tiled with fundamental plaquettes. This gives

$$am_g = -4 \log(b_3/3) + O(b_3^2). \tag{10.23}$$

Using a similar analysis to that for the string tension, Munster (1980) gives the coefficients in this expansion to order b_3^8 .

Including the fermions in the strong coupling expansion is a straightforward procedure. We recall the full action from chapter 7

$$S = \beta \sum_{\square} (1 - (1/n) \text{Re Tr } U_{\square}) + \frac{1}{2} a^3 \sum_{\langle i, j \rangle} \bar{\psi}_i (1 + \gamma_{\mu} e_{\mu}) U_{ij} \psi_j + (a^4 m_0 + 4a^3) \sum_i \bar{\psi}_i \psi_i. \tag{10.24}$$

In the strong coupling limit the gauge fields become random. This suggests treating the second term in eq. (10.24) as a perturbation. This ‘hopping’ term represents the movement of quarks between neighboring sites. Thus we begin with the static quark theory defined by the last term in the action and expand the exponential of the action in powers of the remaining terms. Strictly speaking, the resulting perturbation series is not solely in powers of g_0^{-2} because when a quark–antiquark pair moves as a unit from one site to another, the gauge fields can cancel out, regardless of how random they are. Even in the limit of $g_0^{-2} = 0$, the theory is not exactly solvable and we must make a further expansion. The additional perturbative parameter is effectively the inverse quark mass in units of the lattice spacing.

At this point we introduce sources coupled to the various fields, as discussed in the chapter on fermions. This will allow us to reduce the strong coupling expansion to the manipulation of creation and annihilation operators. We add to the action terms linear in the external sources and in the field variables

$$S_I = S + \sum_i (b_i \psi_i - \bar{\psi}_i c_i) + \sum_{\{ij\}} \text{Tr} (U_{ij} J_{ij} + U_{ji} \bar{J}_{ij}). \quad (10.25)$$

Here b and c are anticommuting sources as discussed in chapter 5. For the gauge variables we introduce matrix valued sources J and \bar{J} analogous to the quantities J and K used in the generating function for group integrals in chapter 8. Now, however, there are independent sources for every link in the lattice. As before, we obtain Green’s functions from derivatives with respect to the sources. We represent these derivatives as creation operators b^+ , c^+ , J^+ , and \bar{J}^+ satisfying the commutation relations

$$[b_i, b_j^+]_+ = \delta_{i,j}, \quad (10.26)$$

$$[c_i, c_j^+]_+ = \delta_{i,j}, \quad (10.27)$$

$$[J_{ij}, J_{kl}^+] = \delta_{i,k} \delta_{j,l}, \quad (10.28)$$

$$[\bar{J}_{ij}, \bar{J}_{kl}^+] = \delta_{i,k} \delta_{j,l}, \quad (10.29)$$

with all other commutators or anticommutators, as appropriate, vanishing. We will turn off the sources by applying them to the ‘empty vacuum’ state satisfying

$$b_i |0\rangle = c_i |0\rangle = J_{ij} |0\rangle = \bar{J}_{ij} |0\rangle = 0. \quad (10.30)$$

We remind the reader that in eqs (10.26–30) we suppress spinor and internal symmetry indices. The site indices indicated explicitly here must not be confused with matrix indices on J and \bar{J} .

As in chapter 5, we define a generating state

$$(W| = (0| \int (d\psi d\bar{\psi} dU) \exp(-S_I). \tag{10.31}$$

Green's functions follow from the formula

$$\begin{aligned} \langle \psi_{i_1} \dots \psi_{i_n} \bar{\psi}_{j_1} \dots \bar{\psi}_{j_n} U_{k_1 l_1} \dots U_{k_m l_m} \rangle \\ = Z^{-1} (W| b_{i_1}^+ \dots b_{i_n}^+ c_{j_1}^+ \dots c_{j_n}^+ J_{k_1 l_1}^+ \dots J_{k_m l_m}^+ |0), \end{aligned} \tag{10.32}$$

where the partition function is simply

$$Z = (W|0). \tag{10.33}$$

Because of the forthcoming analogy with the string model, we call the space in which these creation and annihilation operators act 'string space'. The operator J_{ij}^+ creates a string bit pointing from site i to site j . The source b_i^+ creates an antiquark and c_i^+ a quark at site i . Of course one must not confuse these 'quark' states in string space with states in the physical Hilbert space of the Minkowski world. When we discuss the Hamiltonian formulation of lattice gauge theory, states in the latter space will be distinguished by angular brackets, $|\psi\rangle$.

Strong coupling perturbation theory begins with a breakup of the action into two parts

$$S = S_0 + S', \tag{10.34}$$

where S_0 is the static quark action

$$S_0 = (a^4 m_0 + 4a^3) \sum_i \bar{\psi}_i \psi_i \tag{10.35}$$

and S' contains the remaining terms in eq. (10.24). We now write the generating state in the form

$$(W| = (W_0| \exp(-S'(b^+, c^+, J^+, \bar{J}^+)). \tag{10.36}$$

Here in S' all dependences on ψ , $\bar{\psi}$, and U variables have been replaced with the corresponding source-creation operators. The unperturbed generating state is

$$\begin{aligned} (W_0| = (0| \int (d\psi d\bar{\psi} dU) \exp(-S_0 - \sum_i (b_i \psi_i - \bar{\psi}_i c_i) \\ - \sum_{\{ij\}} \text{Tr}(U_{ij} J_{ij} + U_{ji} \bar{J}_{ij})). \end{aligned} \tag{10.37}$$

Since S_0 is quadratic in the anticommuting fields, the fermionic integral is easily done with a completion of the square

$$\int (d\psi d\bar{\psi}) \exp(-S_0 - \sum_i (b_i \psi_i - \bar{\psi}_i c_i)) = N \exp(-\sum_i b_i (4a^3 + ma^4)^{-1} c_i). \tag{10.38}$$

The irrelevant normalization factor N is just the product over all sites of

$(a^4 m_0 + 4a^3)$. The integral over gauge fields in eq. (10.37) was extensively discussed in chapter 8 for a single link. Thus we have

$$\int (dU) \exp \left(\sum_{\{ij\}} \text{Tr} (U_{ij} J_{ij} + U_{ji} \bar{J}_{ij}) \right) = \prod_{ij} W_G(J_{ij}, \bar{J}_{ij}), \quad (10.39)$$

where W_G is the group-integration generating function of eq. (8.41).

Putting all factors together, we obtain the expression for the generating state

$$\begin{aligned} \langle W | = & \langle 0 | \exp \left(- \sum_i b_i (4a^3 + ma^4)^{-1} c_i \right) \prod_{ij} W_G(J_{ij}, \bar{J}_{ij}) \\ & \times \exp \left(- \frac{1}{2} i a^3 \sum_{\{ij\}} c_i^+ (1 + \gamma_\mu e_\mu) J_{ij}^+ b_j^+ \right) \\ & \times \exp \left(- \beta \sum_{\square} (1 - (1/n) \text{Re Tr} \prod_{\{ij\} \in \square} J_{ij}^+) \right). \end{aligned} \quad (10.40)$$

The strong coupling expansion follows from a power series treatment of the last two terms.

The four terms in eq. (10.40) have a simple interpretation in string space. The first term destroys quark–antiquark pairs at a single site, the second term destroys sets of string bits associated with nearest-neighbor pairs of sites, the third term creates quark–antiquark pairs separated by one lattice spacing and connected by a string bit pointing to the antiquark, and the last term creates elementary squares of string bits. This creation and destruction of quarks and string bits provides the basis of the diagrammatic rules.

Consider some particular Green's function as in eq. (10.32). The graphical rules for calculating this quantity are read off from eq. (10.40):

(1) Draw a set of string bits, quarks, and antiquarks as created by the corresponding operators in eq. (10.32).

(2) Using the third factor in eq. (10.40), create string bits connecting quark–antiquark pairs to produce a configuration where every site has an equal number of quarks and antiquarks. With several types of quarks, each species must balance separately. Closed quark loops can also be generated at this stage. Every quark–string–antiquark combination generated by this rule gives a factor of $\frac{1}{2} i a^3 (1 + \gamma_\mu e_\mu)$ to the amplitude. The spinor indices on these gamma matrices will be contracted in rule (4).

(3) Use the last factor or 'plaquette term' in equation (10.40) to create elementary squares of string bits, thus generating a configuration where every nearest neighbor pairs of sites i, j has a set of string bits which can form a singlet in the gauge group. Thus for $SU(3)$ the number of bits from i to j minus the number from j to i must be a multiple of three. Each plaquette gives a factor of $\beta/6$ to the diagram. A set of m identical plaquettes gives an additional factor of $1/m!$. Alternatively, we can use

the parameters b_R of eq. (10.13) and dress the plaquettes in various representations taken one at a time.

(4) The first term in eq. (10.40) now serves to connect the quark and antiquark lines. They are paired up at each site individually, and in the process spinor, flavor, and the internal symmetry indices of the string bits are contracted. Each such 'quark connection' gives a factor of $(4a^3 + ma^4)^{-1}$ to the amplitude.

(5) At this point we have built up the full diagram. We now begin to tear it down by doing the group integrals. For this purpose we may use the graphical rules from the chapter on group integration. If we are using the parameters b_R , then these integrals proceed as in the discussion of the string tension at the beginning of this chapter.

(6) Some factors of minus one arise from the fermionic nature of the quarks. Each quark line forming an internal closed loop gives a factor of -1 . With the Green's function in the standard ordering of eq. (10.32), if each ψ_{i_k} is connected by a quark line to $\bar{\psi}_{j_k}$, then there are no more factors; otherwise we must multiply by minus one to the number of transpositions necessary to put the ψ 's in the same order as the $\bar{\psi}$'s they are connected to. This is the same rule which gives an ordinary Feynman diagram an extra minus sign for each interchange of external fermion lines.

(7) Sum over all distinct strong coupling diagrams up to the order desired.

(8) Divide by Z , the sum of all vacuum fluctuation diagrams. This will first of all remove contributions of totally disconnected parts of a diagram. In addition, as noted in the discussion of the string tension, non-trivial contributions arise when the vacuum fluctuation overlaps the diagrams in the numerator.

We now illustrate these rules with a simple example. Taking a single quark species, we study

$$\langle \bar{\psi}_i \gamma_5 \psi_i \bar{\psi}_j \psi_j \rangle. \quad (10.41)$$

This is the two-point function for the composite pseudoscalar field $\bar{\psi}_i \gamma_5 \psi_i$. Rule (1) instructs us to place quark–antiquark pairs at site i and site j as illustrated in figure 10.11. In this figure we let the vertical direction represent x_0 and the horizontal direction represent x_1 . In figure 10.12 we show one possible way of applying rule (2), thus adding quark–string–antiquark combinations so as to have all quarks paired with antiquarks. One dressing of the diagram with plaquettes following rule (3) is shown in figure 10.13. Making the quark connections with rule (4) gives figure 10.14. Finally rule (5) is carried out with the repeated use of figure 8.8 to give figure 10.15. Combining the various factors, we obtain the contribution

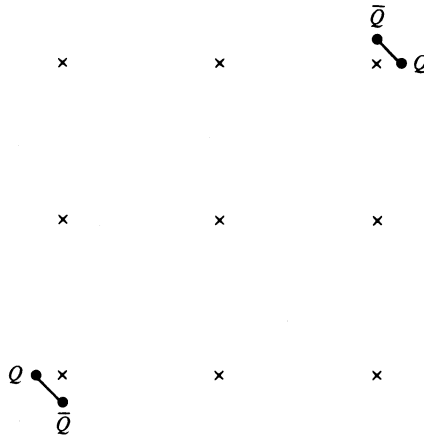


Fig. 10.11. The quark–antiquark pairs created by the correlation function in eq. (10.41) (Creutz, 1978a).

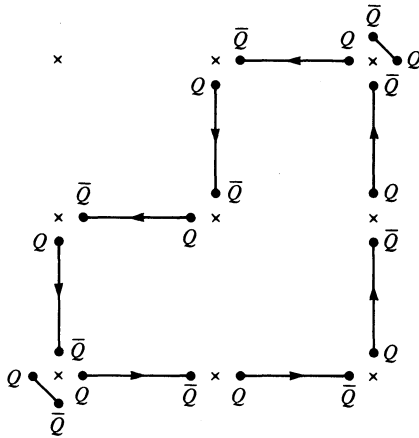


Fig. 10.12. A set of quark–string–antiquark combinations pairing all quarks with antiquarks (Creutz, 1978a).

of this diagram to the amplitude

$$(ia^3)^8 \left(\frac{\beta}{6}\right)^3 (4a^3 + ma^4)^{-10} 3^{-2} \text{Tr } \Gamma, \tag{10.42}$$

where Γ is the product of the Dirac operators around the diagram

$$\begin{aligned} \text{Tr } \Gamma &= 2^{-8} \text{Tr} (\gamma_5(1 + \gamma_0)(1 + \gamma_1)(1 + \gamma_0)(1 + \gamma_1), \\ &\gamma_5(1 - \gamma_0)^2(1 - \gamma_1)^2) = \frac{1}{4}. \end{aligned} \tag{10.43}$$

Note that eq. (10.42) can be put in the form

$$3(4a^3 + ma^4)^{-2} \text{Tr } \Gamma (4 + ma)^{-p} (\beta/18)^A, \tag{10.44}$$

quark ‘hops’ from site to site as in rule (2) we pick up a factor of

$$i(4+ma)^{-1}\frac{1}{2}(1+\gamma_\mu e_\mu) = iK_h(1+\gamma_\mu e_\mu). \quad (10.45)$$

In a naive continuum limit the ‘hopping constant’ K_h goes to $1/8$. At finite lattice spacing, the critical value of K_h representing vanishing bare quark mass can be substantially renormalized through interactions. The strong coupling expansion is effectively in powers of β and K_h .

Equation (10.44) generalizes to all diagrams with the same topology as the diagram in figure 10.14, that is all diagrams with a single surface of plaquettes bounded by a quark line. This shows the striking connection between Wilson’s theory and an oriented string model where the action

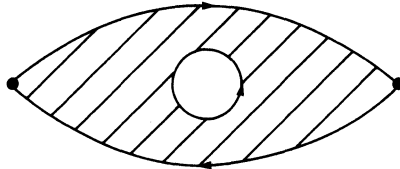


Fig. 10.16. A class of diagrams contributing to meson propagators (Creutz, 1978a).

associated with a particular world sheet swept out by a string contains a term proportional to its area. In the strong coupling limit, the effective tension K in the string is the same quantity evaluated at the beginning of this chapter. In two-dimensional space-time this connection with the string model can be made precise (Bars, 1976). In four dimensions the picture is not the simple string model (Goddard *et al.*, 1973) due to complicated interstring interactions arising in higher orders (Weingarten, 1980).

The string analogy provides a useful topological classification of strong coupling diagrams. For example, a prototype diagram contributing to the pseudoscalar two-point function of eq. (10.41) is illustrated in figure 10.16. In this diagram the world sheet built up of plaquettes has a hole rimmed with a quark loop. The result for such a diagram is

$$-\frac{1}{3}(4a^3+ma^4)^{-2} \text{Tr}(\Gamma_E) \text{Tr}(\Gamma_I) (4+ma)^{-p} (\beta/18)^A, \quad (10.46)$$

where Γ_E is the product of the Dirac matrices around the external loop, and Γ_I is a similar product around the internal loop. Here the perimeter p is again the total quark line length and includes both the fermionic loops. The factor of $1/3$ in front of this expression represents the basis of the $1/n$ topological expansion (t’Hooft, 1974). Each additional quark loop inserted into a world sheet of a string will give another factor of $1/3$. In figure 10.17 we show a class of diagrams contributing to baryon structure. In strongly

coupled lattice gauge theory, the proton consists of three quarks at the end of strings connected in a 'Y' configuration.

As mentioned above, the strong coupling expansion is a simultaneous series in g_0^{-2} and K_h . In particular, the limit of infinite g_0^2 or vanishing β with K_h remaining finite is not exactly solvable. In this extreme, no plaquettes can be generated. Consequently, the two quarks of a meson must hop from

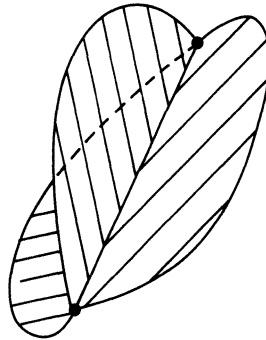


Fig. 10.17. A class of strong coupling diagrams contributing to baryon propagation (Creutz, 1978a).

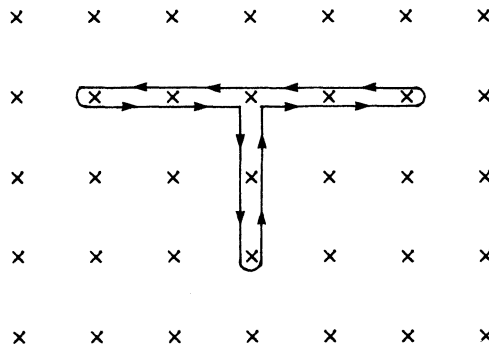


Fig. 10.18. A diagram giving a non-vanishing three-point function even in the limit of infinite g_0^2 .

site to site together. Nevertheless, the hadrons are not free particles because they can still exchange these zero radius mesons. For example, we have non-vanishing three-point vertices of the type illustrated in figure 10.18. Although one should not expect a great deal of detailed phenomenological success, this limit has received considerable attention as an interesting simplification for the study of chiral symmetry breaking in a confining theory.

t'Hooft (1980) has suggested that there is an intimate connection between confinement and the phenomenon of chiral symmetry breaking. He argued that there are strong constraints which must be satisfied if a confining theory has massless bare fermion constituents and does not have massless Goldstone bosons associated with the chiral symmetry. The problem arises from the analytic structure of a three-point vertex constructed from two vector and one axial vector currents. The anomaly requires this object to be non-analytic at zero momentum transfer through the three channels. This requires real intermediate states of vanishing physical mass. In a confining theory these could be either Goldstone bosons or massless baryons. Further arguments (Coleman and Witten, 1980; Banks *et al.*, 1980) indicate the impossibility of the latter case in many theories, probably including the $SU(3)$ theory of the strong interactions.

This situation appears to carry over to the strongly coupled lattice theory. Such investigations require some treatment of the doubling problems alluded to in chapter 5. As the infinite g_0^2 theory with finite K_h is not exactly solvable, further approximations such as large dimension (mean field theory) or large gauge group are needed. The results of these calculations are strong indications that the theory adopts the broken symmetry alternative with massless 'pions' and an expectation value for the order parameter $\bar{\psi}\psi$ (Blairon *et al.*, 1981; Kluberg-Stern *et al.*, 1981; Svetitsky *et al.*, 1980).

Problems

1. Evaluate the diagram in figure 10.3 and show that it indeed gives a perimeter law.
2. Does strongly coupled $SO(3)$ lattice gauge theory confine in the sense of having a mass gap?